ELSEVIER

Materials Science and Engineering A192/193 (1995) 92–96

MATERIALS SCIENCE & ENGINEERING A

Dislocation structure in $L1_2$ Mn-stabilized Al_3Ti deformed between 77 and 873 K

Joël Douin[a], K. Sharvan Kumar[b], Patrick Veyssière[a]

[a]*LEM, CNRS-ONERA, BP 72, 92322 Châtillon Cedex, France*

[b]*Martin Marietta Laboratories, 1450 South Rolling Road, Baltimore, MA 21227, USA*

Abstract

Polycrystalline samples of $L1_2$ Mn-stabilized Al_3Ti were deformed in compression from low temperature to the temperature of the flow stress plateau. The fine structure of the superdislocations was analyzed under weak-beam conditions with particular attention paid to the operating glide systems at different temperatures. The dissociation mode of the dislocations was also addressed in order to discriminate between antiphase boundary-coupled dislocations and Superlattice Intrinsic Stacking Fault (SISF)-coupled partial dislocations. The existence of a strong Peierls effect on undissociated ⟨110⟩ dislocations during deformation at 573 K is reported, as well as the observation at low temperature of dislocations with ⟨100⟩ and ⟨112⟩ Burgers vectors.

Keywords: Dislocation; Manganese; Aluminium; Titanium; Deformation

1. Introduction

Trialuminide alloys based on Al_3Ti have the potential for use in aerospace applications. These alloys possess good strength, combined with low density and good oxidation resistance, and are expected to exhibit specific properties superior to Ni-based superalloys [1,2]. Unfortunately, due to their tetragonal $D0_{22}$ structure, they are very brittle, and this is currently ascribed to a lack of a sufficient number of slip systems [3]. $D0_{22}$-Al_3Ti can be transformed to the related cubic $L1_2$ structure, which allows for more slip systems, by the addition of ternary elements, such as Fe, Cr or Mn [4,5]. This has been proposed as a possible route to improve the ductility of Al_3Ti-based alloys.

In this study, we address the microstructural properties of the $L1_2$ Mn-based compound $Al_{66}Ti_{25}Mn_9$ whose remarkable mechanical properties include a plateau of the temperature dependence of the flow stress between 500 and 1000 K [6] and some ductility at ambient temperature. We focus on the analysis of the fine structure of dislocations in relation to deformation mechanisms. Special attention is paid to the dissociation modes and operative glide systems as the deformation temperature is varied.

2. Experimental procedure

The preparation of $L1_2$-$Al_{66}Ti_{25}Mn_9$ has been described by Kumar et al. [6]. It should be emphasized that, prior to mechanical testing, this compound was isothermally forged at 1383 K. The samples examined in this study were deformed in compression at a strain rate of 2×10^{-4} s^{-1} at 77, 573 and 873 K to a permanent strain between 1.1% and 1.8%. Thin foils for transmission electron microscopy were prepared by electropolishing in a solution of 20% nitric acid in methanol maintained at 240 K and at a voltage of 12 V (60 mA).

3. Results

3.1. Deformation at 77 K

A typical area of a sample deformed at 77 K is shown in Fig. 1. Three different types of dislocations (a, b and c) are observed, which have ⟨110⟩, ⟨100⟩ and, unexpectedly, ⟨112⟩ Burgers vectors respectively. They all adopt configurations suggesting that they are at least slightly mobile during deformation.

SSDI 0921-5093(94)03209-2

⟨110⟩ dislocations usually adopt curved configurations. They are dissociated into two like $\frac{1}{2}\langle 110\rangle$ superpartials separated by an antiphase boundary (APB) (Fig. 1, segments a). The ⟨110⟩ dislocations are, in general, dissociated in their {111} slip plane. More complex configurations can, however, be observed. Fig. 2 shows an example of a [110] dislocation perfectly aligned with the $[12\bar{1}]$ direction. $\boldsymbol{g}\cdot\boldsymbol{b}$ contrast experiments demonstrate unambiguously that this particular dislocation is dissociated into two like $\frac{1}{2}[110]$ APB-coupled superpartials. In addition, tilting experiments show that segment 1 is fully dissociated in the $(\bar{1}11)$ glide plane, whereas segment 2 has adopted a dihedral configuration (Fig. 2(f)). While mainly dissociated in the (101) plane, which is not its glide plane, segment 2 is also partly extended in the $(\bar{1}11)$ plane (see arrows). It should be noted that, under some imaging conditions, an oscillating contrast (which arises from the inclination of any defect in a foil) decorates segment 1 as a fringe-containing dislocation, which may be incorrectly interpreted as a stacking fault contrast (Fig. 2(e)). In addition, we confirm the presence of a strong residual contrast of the APB under conditions wherein it should be invisible, as previously reported in $D0_{22}$-Al_3Ti [7] and in $L1_2$ alloys [8,9]. This is probably a manifestation of the occurrence of some relaxation process at the APB which induces an additional displacement vector. The disso-

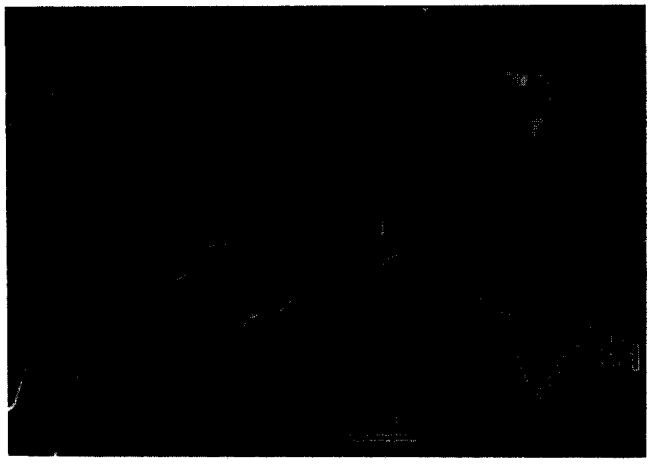

Fig. 1. Dislocations in Al–Ti–Mn deformed at 77 K. Dislocations a, b and c have ⟨110⟩, ⟨100⟩ and ⟨112⟩ Burgers vectors respectively; beam direction (BD), [101].

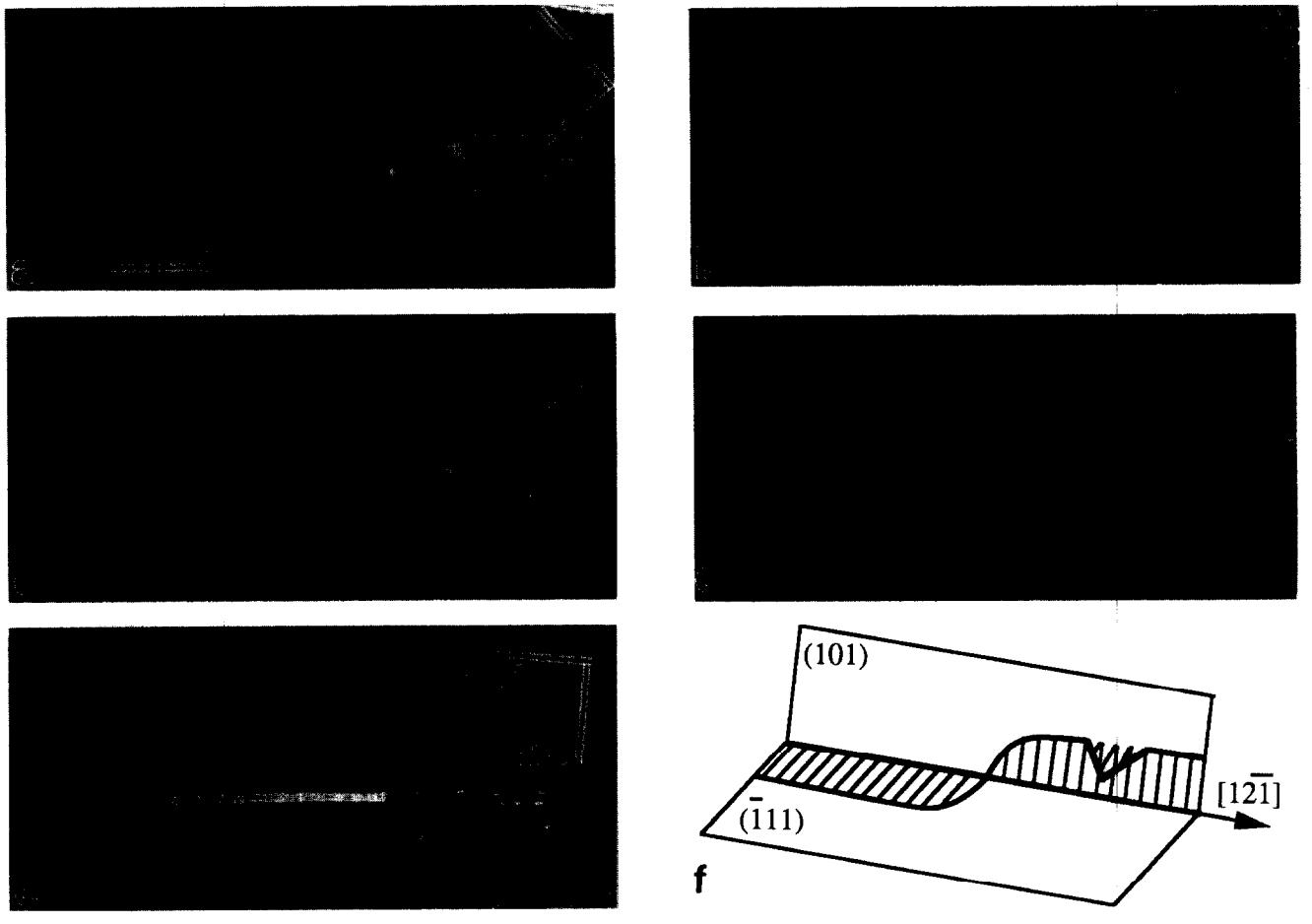

Fig. 2. [110] dislocations observed after deformation at 77 K. (a, b) BD = [001]; (c, d) BD = [011] (notice the residual contrast for extinction with the $1\bar{1}1$ reflection); (e) BD = [112]; (f) schematic diagram of the configuration.

ciation distances are 13 ± 2 nm and 10 ± 1.5 nm for $(\bar{1}11)$ and (101) respectively. This would correspond to APB energies $\gamma_{\{111\}} = 100 \pm 20$ mJ m^{-2} and $\gamma_{\{110\}} = 135 \pm 20$ mJ m^{-2} (calculated using isotropic elasticity, with $\mu = 80$ GPa and $\nu = 1/3$ [10,11] and a cell parameter of 0.366 nm).

$\langle 100 \rangle$ dislocations are present in samples deformed at 77 K (Fig. 1, segments b; Fig. 3). They are preferentially aligned along the $\langle 110 \rangle$ directions in their $\{001\}$ glide plane, as in Ni_3Al in which they have been found to exhibit a strong preference for the 45° character as a consequence of elastic anisotropy [12]. No dissociation of these dislocations has been observed even under the extreme $\boldsymbol{g}$–$6\boldsymbol{g}$ weak-beam conditions. Since no slip traces indicative of the $\langle 100 \rangle \{001\}$ glide system have been reported [13], these dislocations should contribute very little to the total amount of deformation. The low mobility of $\langle 100 \rangle$ dislocations may originate from the occurrence of a large number of pinning points on their lines (Fig. 3), which would prevent them from moving over large distances. There also exists a large friction stress acting on $\langle 100 \rangle$ dislocations, as indicated by the unrelaxed bowing of the lines between the pinning points, the origin of which has not yet been elucidated.

$\langle 112 \rangle$ dislocations are also observed after deformation at 77 K. They result from the interaction of $\langle 110 \rangle$ dislocations according to

$$[110] + [011] \rightarrow [121]$$

Their dissociation schemes and formation mode are complex and will be analyzed elsewhere [14].

Reasons for the coexistence of these three families of dislocations are reported in Section 4.

3.2. Deformation at 573 K

The microstructures observed after deformation at 573 K are quite straightforward. No $\langle 112 \rangle$ dislocations have been detected so far at this temperature and the presence of $\langle 100 \rangle$ dislocations is uncertain. Only the $\langle 110 \rangle \{111\}$ slip system is active during deformation (Fig. 4). The main feature is the occurrence of abrupt changes in direction lines along the $\langle 110 \rangle$ directions of the slip plane. This highly segmented shape of $\langle 110 \rangle$ dislocations is indicative of a strong stabilization effect along the Peierls valleys.

A major fraction of the dislocations are observed to be undissociated, as in $L1_2$ Ni-stabilized Al_3Ti [15]. Also, as observed by Morris and Lerf [16] in Fe-modified titanium trialuminide, some of the dislocations are seen to consist of successively dissociated and undissociated segments. When dissociated, the $\frac{1}{2}\langle 110 \rangle$ superpartials are separated only by a very small distance, of the order of 1 nm. Again, no stacking fault fringes or dissociation of $\langle 110 \rangle$ dislocations into two $\frac{1}{3}\langle 112 \rangle$ superpartials has been observed.

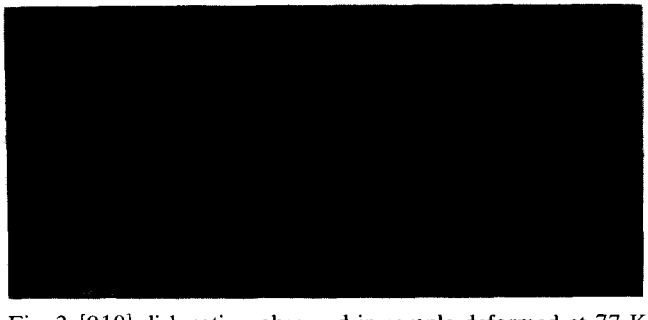

Fig. 3. [010] dislocation observed in sample deformed at 77 K (notice the numerous pinning points and the curvature of the dislocation between them); BD = [101].

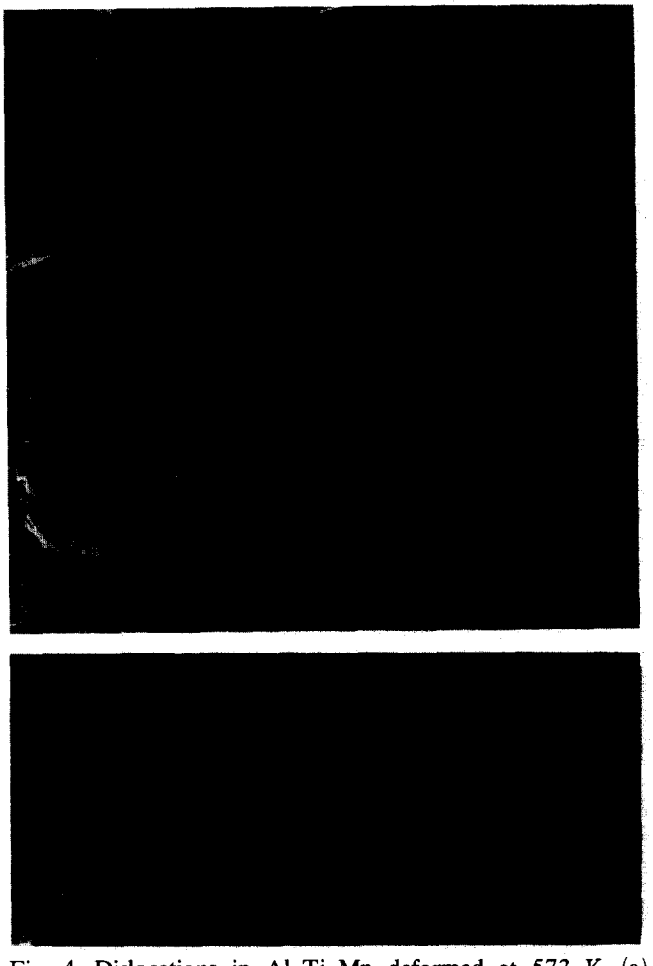

Fig. 4. Dislocations in Al–Ti–Mn deformed at 573 K. (a) BD = [011] (notice the strong segmentation of the dislocations along the three $\langle 110 \rangle$ directions of the $(\bar{1}11)$ plane, i.e. $[0\bar{1}1]$, [110] and [101] ($[2\bar{1}\bar{1}]$ and $[2\bar{1}1]$ are the projections on (011) of [110] and [101] respectively)); (b) enlargement of the same area showing a single [110] dislocation with lines along the three $\langle 110 \rangle$ directions of the $(\bar{1}11)$ plane.

3.3. Dissociation at 873 K

After deformation at high temperature, the dominant glide system remains as $\langle 110 \rangle \{111\}$ (Fig. 5). Compared with deformation at 573 K, the dislocations adopt very smooth configurations. $\langle 110 \rangle$ dislocations are much more widely dissociated, yet APB-coupled. Screw dislocations are dissociated in the $\{001\}$ plane as a result of the operation of the Kear–Wilsdorf process, but climb dissociation is also observed at non-screw segments. This is exemplified in Fig. 5 where the projected APB width of curved dislocations varies with line orientation. Dislocation c in Fig. 5 has a [110] Burgers vector with line directions along [001] and $[11\bar{2}]$. It is almost pure edge in character, and tilting experiments have demonstrated that it is dissociated by climb in the $(1\bar{1}0)$ plane. It is worth recalling that climb dissociation minimizes the interaction energy between superpartials as soon as the dislocation exhibits some edge component: when the APB energy does not vary significantly with orientation, companion superpartials will lie on a plane perpendicular to their slip plane, as for dislocation c in Fig. 5.

$\langle 100 \rangle$ dislocations are also observed in places (Fig. 6). They present exactly the same features as those observed in samples deformed at 77 K, i.e. they usually have a mixed 45° character and appear to be trapped at potent pinning points.

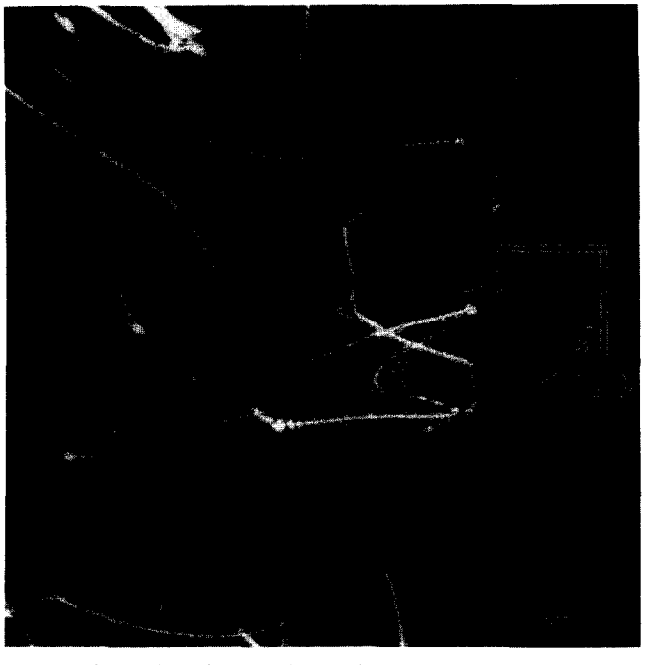

Fig. 5. Dislocations in Al–Ti–Mn deformed at 873 K. Dislocations a, b and c have $[01\bar{1}]$, $[1\bar{1}0]$ and [110] Burgers vectors respectively.

4. Discussion and conclusions

Before attempting to relate the observed microstructures to the deformation mechanisms, we will discuss the relevance of our observations on samples deformed at low temperatures.

From a consideration of the foils deformed at 77 K, there is a strong indication that the microstructure is greatly affected by the isothermal forging of the samples prior to mechanical testing. In particular, the observation of $\langle 100 \rangle$ dislocations in samples deformed at 77 K is intriguing. This could originate from the fact that deformation is reminiscent of the parent $D0_{22}$ alloy where $\langle 100 \rangle$ dislocations are about as frequent as $\langle 110 \rangle$ dislocations and where they contribute significantly to deformation, as in Al_3X alloys with X ≡ Ti, V or Nb [15,17–19]. In the present alloy, this does not appear to be the case, since these dislocations are strongly pinned, nor do they seem to be due to the decomposition of $\langle 110 \rangle$ dislocations, as observed in $D0_{22}$-Al_3Ti [7]. An analogy with $L1_2$ alloys does not work either, since we have no evidence for the formation of $\langle 100 \rangle$ segments as a result of the intersection of two dissociated $\langle 110 \rangle$ dislocations, as observed in Ni_3Al [12]. Since $\langle 100 \rangle$ dislocations adopt the same configuration after deformation at both 77 K and 873 K, we believe that they are formed during the isothermal forging prior to the mechanical testing, i.e. under high-temperature conditions. They would be so strongly immobilized by pinning points that they could not be eliminated on subsequent deformation. It should be noted that, in $L1_2$ alloys, the $\langle 100 \rangle \{001\}$ glide system operates at high temperatures [20–22].

In samples deformed at 77 K, the observation of $\langle 110 \rangle$ dislocations dissociated in the $\{110\}$ plane (Fig. 2) should be ascribed to high-temperature deformation: climb dissociation operates at 873 K and dissociation of pure edge $\langle 110 \rangle$ dislocations in $\{110\}$ planes seems to be quite a common feature at high temperature (Fig. 5). In the case of Fig. 2, the incomplete configuration is due to the incomplete transformation of the high-temperature configuration (dissociation plane

Fig. 6. [010] dislocations found after deformation at 873 K (notice the similarity to the configuration in Fig. 3).

(101), resulting from deformation at 873 K) into the stable configuration at 77 K (dissociation in $(\bar{1}11)$ plane) on application of a stress. This explanation, based on the existence of climb dissociated dislocation prior to deformation at 77 K, holds true for the formation of $\langle 112 \rangle$ dislocations [14].

We now address the correlation between microstructures and deformation mechanisms.

Firstly, it should be emphasized that no SISF-coupled $\langle 110 \rangle$ dislocations were observed during this study. There has been a lot of controversy regarding the rate-controlling dissociation mode in the cubic Al_3Ti alloys (see, for example, Refs. [23] and [24]), and our study confirms that in Mn-modified Al_3Ti superdislocations are APB-coupled.

Secondly, the strong line segmentation of dislocations after deformation at 573 K indicates that deformation is controlled by a Peierls mechanism. The fact that high Peierls forces along close-packed directions might determine the (negative) temperature dependence of the stress has already been suggested in the case of Co_3Ti [25]. Still, $\langle 110 \rangle$ dislocations must be quite mobile in order to provide a tensile ductility of about 1% at this temperature [6].

Finally, it is sometimes argued that the lack of ductility results from the fact that when $\langle 110 \rangle$ dislocations are not dissociated they are submitted to a large friction force from the lattice. Their poor mobility would impede stress relaxation by dislocation emission from crack tips [26]. This argument does not seem to hold true in $Al_{66}Ti_{25}Mn_9$, since the separation between partials increases dramatically with increasing temperature from 573 to 873 K, while the ductility decreases in the same range (the tensile elongation reduces from 1.0% at 600 K to 0.3% at 800 K, see fig. 5 of Ref. [6]). In addition, it has been shown that a material may be brittle at room temperature despite the fact that dislocations are dissociated [27].

Acknowledgment

One of the authors (K.S.K.) was supported by the NASA Lewis Research Center under Contract No. NAS3-25787 during the time in which the material was processed and tested.

References

[1] K.S. Kumar, *Int. Met. Rev., 35* (1990) 293.
[2] D.P. Pope, in O. Izumi (ed.), *Intermetallic Compounds—Structure and Mechanical Properties*, Japan Institute of Metals, Sendai, 1991, p. 301.
[3] M. Yamaguchi, Y. Umakoshi and T. Yamane, *Philos. Mag. A, 55* (1987) 301.
[4] K.S. Kumar and J.R. Pickens, *Scr. Metall., 22* (1988) 1015.
[5] S. Zhang, J.P. Nic and D.E. Mikolla, *Scr. Metall., 24* (1990) 57.
[6] K.S. Kumar, S.A. Brown and J.D. Whittenberger, in L.A. Johnson, D.P. Pope and J.O. Stiegler (eds.), *High Temperature Ordered Intermetallic IV, MRS Proc. 213*, Materials Research Society, Pittsburgh, 1991, p. 481.
[7] G. Hug, J. Douin and P. Veyssière, in C.T. Liu, A.I. Taub, N.S. Stoloff and C.C. Koch (eds.), *High Temperature Ordered Intermetallic III, MRS Proc. 133*, Materials Research Society, Pittsburgh, 1988, p. 125.
[8] J. Douin and P. Veyssière, *Philos. Mag. A, 64* (1991) 807.
[9] D.G. Morris, in C.T. Liu, R.W. Cahn and G. Sauthoff (eds.), *Ordered Intermetallics—Physical Metallurgy and Mechanical Behaviour*, Kluwer Academic, Dordrecht, 1991, p. 123.
[10] C.D. Turners, W.O. Powers and J.A. Wert, *Acta Metall. Mater., 37* (1989) 2635.
[11] R. Lerf and D.G. Morris, *Acta Metall. Mater., 39* (1991) 2419.
[12] P. Veyssière and J. Douin, *Philos. Mag. Lett., 51* (1985) 1.
[13] S.A. Brown, D.P. Pope and K.S. Kumar, in I. Baker, R. Darolia, J.D. Whittenberger and M.H. Yoo (eds.), *High Temperature Ordered Intermetallic V, MRS Proc. 288*, Materials Research Society, Pittsburgh, 1993, p. 723.
[14] J. Douin, in preparation.
[15] V. Vasudevan, R. Wheeler and H.L. Fraser, in C.T. Liu, A.I. Taub, N.S. Stoloff and C.C. Koch (eds.), *High Temperature Ordered Intermetallic III, MRS Proc. 133*, Materials Research Society, Pittsburgh, 1988, p. 705.
[16] D.G. Morris and R. Lerf, in L.A. Johnson, D.P. Pope and J.O. Stiegler (eds.), *High Temperature Ordered Intermetallic IV, MRS Proc. 213*, Materials Research Society, Pittsburgh, 1991, p. 305.
[17] D. Shechtman and L.A. Jacobson, *Metall. Trans. A, 6* (1975) 1325.
[18] A. François, *Ph.D. Thesis*, University of Paris VI, 1992.
[19] D.G. Morris and R. Lerf, *Philos. Mag. A, 63* (1991) 1195.
[20] P.M. Hazzledine, M.H. Yoo and Y.Q. Sun, *Acta Metall., 37* (1989) 3235.
[21] Y.Q. Sun, *Ph.D. Thesis*, University of Oxford, 1990.
[22] N. Baluc, *Ph.D. Thesis*, University of Lausanne, 1990.
[23] H. Inui, D.E. Luzzi, W.D. Porter, D.P. Pope, V. Vitek and M. Yamaguchi, *Philos. Mag. A, 65* (1992) 245.
[24] P. Veyssière and D.G. Morris, *Philos. Mag. A, 67* (1993) 491.
[25] J. Oliver, *Ph.D. Thesis*, University of Paris-Sud, 1992.
[26] C.D. Turner, W.O. Powers and J.A. Wert, *Acta Metall., 37* (1989) 2635.
[27] E.P. George, J.A. Horton, W.D. Porter and J.H. Scneibel, *J. Mater. Sci., 5* (1990) 1639.